Predicting Meridian in Chinese Traditional Medicine Using Machine Learning Approaches

Yinyin Wang[1], Mohieddin Jafari[1], Yun Tang[2] and Jing Tang[1,3*]

[1]Research Program in Systems Oncology, Faculty of Medicine, University of Helsinki, 00290, Finland

[2]Shanghai Key Laboratory of New Drug Design, School of Pharmacy, East China University of Science and Technology, Shanghai, 200237, China

[3]Institute for Molecular Medicine Finland, Helsinki Institute of Life Science, University of Helsinki, 00290, Finland

*Corresponding author: Jing Tang, jing.tang@helsinki.fi

Abstract

Plant-derived nature products, known as herb formulas, have been commonly used in Traditional Chinese Medicine (TCM) for disease prevention and treatment. The herbs have been traditionally classified into different categories according to the TCM Organ systems known as Meridians. Despite the increasing knowledge on the active components of the herbs, the rationale of Meridian classification remains poorly understood. In this study, we took a machine learning approach to explore the classification of Meridian. We determined the molecule features for 646 herbs and their active components including structure-based fingerprints and ADME properties (absorption, distribution, metabolism and excretion), and found that the Meridian can be predicted by machine learning approaches with a top accuracy of 0.83. We also identified the top compound features that were important for the Meridian prediction. To the best of our knowledge, this is the first time that molecular properties of the herb compounds are associated with the TCM Meridians. Taken together, the machine learning approach may provide novel insights for the understanding of molecular evidence of Meridians in TCM.

Author Summary

In East Asia, plant-derived natural products, known as herb formulas, have been commonly used as Traditional Chinese Medicine (TCM) for disease prevention and treatment. According to the theory of TCM, herbs can be classified as different Meridians according to the balance of Yin and Yang, which are commonly understood as metaphysical concepts. Therefore, the scientific rational of Meridian classification remains poorly understood. The aim of our study was to provide a computational means to understand the classification of Meridians. We showed that the Meridians of herbs can be predicted by the molecular and chemical features

of the ingredient compounds, suggesting that the Meridians indeed are associated with the properties of the compounds. Our work provided a novel chemoinformatics approach which may lead to a more systematic strategy to identify the mechanisms of action and active compounds for TCM herbs.

1. Introduction

Single-agent drug discovery has often experienced low success rates which can be largely attributed to the lack of efficacy as well as unsatisfactory safety, especially when treating complex diseases such as cancer [1] and diabetes [2]. Recently, polypharmacology that involves multi-drug combinations acting on distinct targets has been proposed as a paradigm shift of drug discovery [3]. However, without a systems-level understanding of disease and drug interactions, it maintains a challenge to develop a valid strategy for the rational selection of drug combinations. In East Asia, plant-derived natural products, known as herb formulas, have been commonly used in Chinese Traditional Medicine (TCM) for disease prevention and treatment. Herb formulas often involve multiple bioactive components to produce synergistic effects in a personalized medicine manner, aiming for maximal therapeutic efficacy as well as minimal side effects [4]. For example, the Fufang Danshen Diwan (*Dantonic pill*), a botanical drug consisting of extracts of Danshen (*Radix Salviae Miltiorrhizae*) and Sanqi (*Radix Notoginseng*) is currently approved in 26 countries outside the USA for the treatment and prevention of chronic stable angina pectoris and other cardiovascular disease related conditions [5]. In this regard, understanding the bioactive components and their mechanisms of action for herb formulas might provide important insights on the rational design of multi-drug combinations for complex diseases [6, 7].

The prescription of herb formulas in TCM has been based on a holistic principle to model the human body as a miniature system that resemble the universe, which is composed

of five interacting Elements (metal, wood, water, fire and earth)[8]. Similar to other schools of systems medicine, the cause of diseases or symptoms can be perceived as the loss of balance between these Five Elements [9, 10]. Treating a given disease is therefore equivalent to restoring the balance in the system [11], which can be achieved by either acupuncture [12, 13] or herb formulas that tune specifically certain inner channels of the body, known as Meridians [14]. There are 12 principal Meridians, each of which is linked to a specific TCM Organ and can be further attributed to one of the Five Elements (**Table 1**). The concept of Organ in TCM is fundamentally different from that of modern anatomic perspective, as the Organs in TCM represent certain distinct states of the human body, rather than a morphological structure. Similarly, although the Meridian system has been established as a fundamental basis of TCM several thousand years ago, it is not coincided to the known patterns of blood vessels or central nervous system [15]. More recently, fascia networks [16] and perivascular space [17] have been proposed to explain Meridian, but neither of them have been experimentally confirmed.

Table 1. The Meridians and their example herbs. Each Meridian is linked to a particular Organ which is characterized by its Elements and Quality of Yin or Yang. TCM considers a disease a result of loss of balance in the Yin and Yang, which can be restored using herbs that target particular Meridians.

Meridian name	Quality of Yin or Yang	Main organ	Example Herb
Taiyin **Lung** Channel of Hand	Greater Yin (taiyin)	Lung	Rhizoma Pinelliae
Shaoyin **Heart** Channel of Hand	Lesser Yin (shaoyin)	Heart	Salvia miltiorrhiza
Jueyin **Cardiovascular** Channel of Hand	Faint Yin (jueyin)	Cardiovascular	Motherwort Herb
Hand's Minor Yang **Three End**	Lesser Yang (shaoyang)	Three End	Cape jasmine fruit
Taiyang **Small Intestine** Channel of Hand	Greater Yang (taiyang)	Small Intestine	Adsuki Bean
Yangming **Large Intestine** Channel of Hand	Yang Bright (yangming)	Large Intestine	Radix et rhizoma rhei
Taiyin **Spleen** Channel of Foot	Greater Yin (taiyin)	Spleen	Pueraria Root
Shaoyin **Kidney** Channel of Foot	Lesser Yin (shaoyin)	Kidney	Radix Angelicae Biseratae
Jueyin **Liver** Channel of Foot	Faint Yin (jueyin)	Liver	Bupleurum chinense DC
Shaoyang **Gallbladder**	Lesser Yang (shaoyang)	Gall Bladder	Spica Prunellae
Taiyang **Bladder** Channel of Foot	Greater Yang (taiyang)	Urinary bladder	Common Andrographis Herb
Yangming **Stomach** Channel of Foot	Yang Bright (yangming)	Stomach	Rhizoma Cyperi

While the anatomical and physiological evidence of Meridians are yet to be determined, the narrative of TCM allows for the classification of herb formulas based on their targeting Meridians [18-20]. The rationale of Meridian has been investigated for a few TCM herbs. For example, Jie Geng (*Platycodi Radix*) has been considered as a Lung Meridian herb, and it was discovered recently that an active ingredient in Jie Geng called saponin can affect the lung and respiratory systems by the inhibition of lipid peroxidation [21]. Another example is Danshen, the dried root of *Salvia miltiorrhiza burge*, which has been used for treating cardiovascular diseases and hepatitis as a Heart and Liver Meridian herb [22]. Recent studies have shown that its lipophilic ingredients such as tanshinones and hydrophilic ingredients such as salvianic acids may play a synergistic role to achieve its therapeutic efficacy [23]. With the increasing knowledge about the biochemical and pharmacological properties of the bioactive ingredients from the TCM herbs, it is now possible to carry out a larger-scale analysis to investigate the molecular basis of Meridians and other concepts in TCM [24].

To leverage the complex biochemical and pharmacological datasets, systems biology approaches involving machine learning techniques have been utilized to the study of herb

formulas [25]. For example, Fu *et al.* developed a data clustering method using a collection of 2,012 compounds associated with TCM herbs and discovered that the hot or cold nature of the herbs can be correlated with the physicochemical and target pathways of their ingredient compounds [26]. Wang *et al.* collected 5,464 compounds for 115 herbs and applied an unsupervised clustering method called Self-organizing map (SOM) to establish a classifier of cold and hot herbs based on the chemical structural fingerprints of the compounds [27]. However, these machine learning studies focused only on the hot/cold classification of TCM herbs, while it remains unknown whether the Meridian classification that involves 12 major classes can be also predicted from the chemical structure and physiochemical features of ingredient compounds.

In this study, we collected the Meridian information of herbs as well as the chemical structures of their ingredient compounds. These two datasets were utilized to determine the molecular features including structure-based fingerprints and ADME properties. With the feature matrices determined at both the herb level and the compound level, we further developed a machine learning framework to predict the Meridians of the herbs and their ingredient compounds. We tested multiple machine learning methods and showed that the classification of Meridians can be predicted especially at the compound level. These results suggested that Meridians indeed are associated with the molecular properties of herb compounds. We expected that our data integration approach may represent a novel perspective for the understanding of Meridian, which may ultimately lead to a more systematic exploration of the mechanisms of TCM.

2. Materials and Methods

The entire workflow of the present study was illustrated in **Fig 1**. First, herbs and their ingredient compounds were extracted from public databases. Molecular fingerprints and ADME properties were determined based on the chemical structures of the ingredient

compounds, and were used to construct an Herb-feature matrix and a Compound-Meridian matrix. After obtaining all the features and Meridian classification for the herbs and the compounds, the prediction of Meridians at the herb and compound levels was implemented using four machine learning methods, including Support vector machine (SVM) [28], Decision tree (DT) [29], Random forests (RF) [30, 31] and K-nearest neighbor (kNN) [32]. The predication performance was further evaluated by cross-validation, based on which we identified the best models and feature types to predict the Meridians. The most predictive fingerprint features and ADME properties were identified for each Meridian separately.

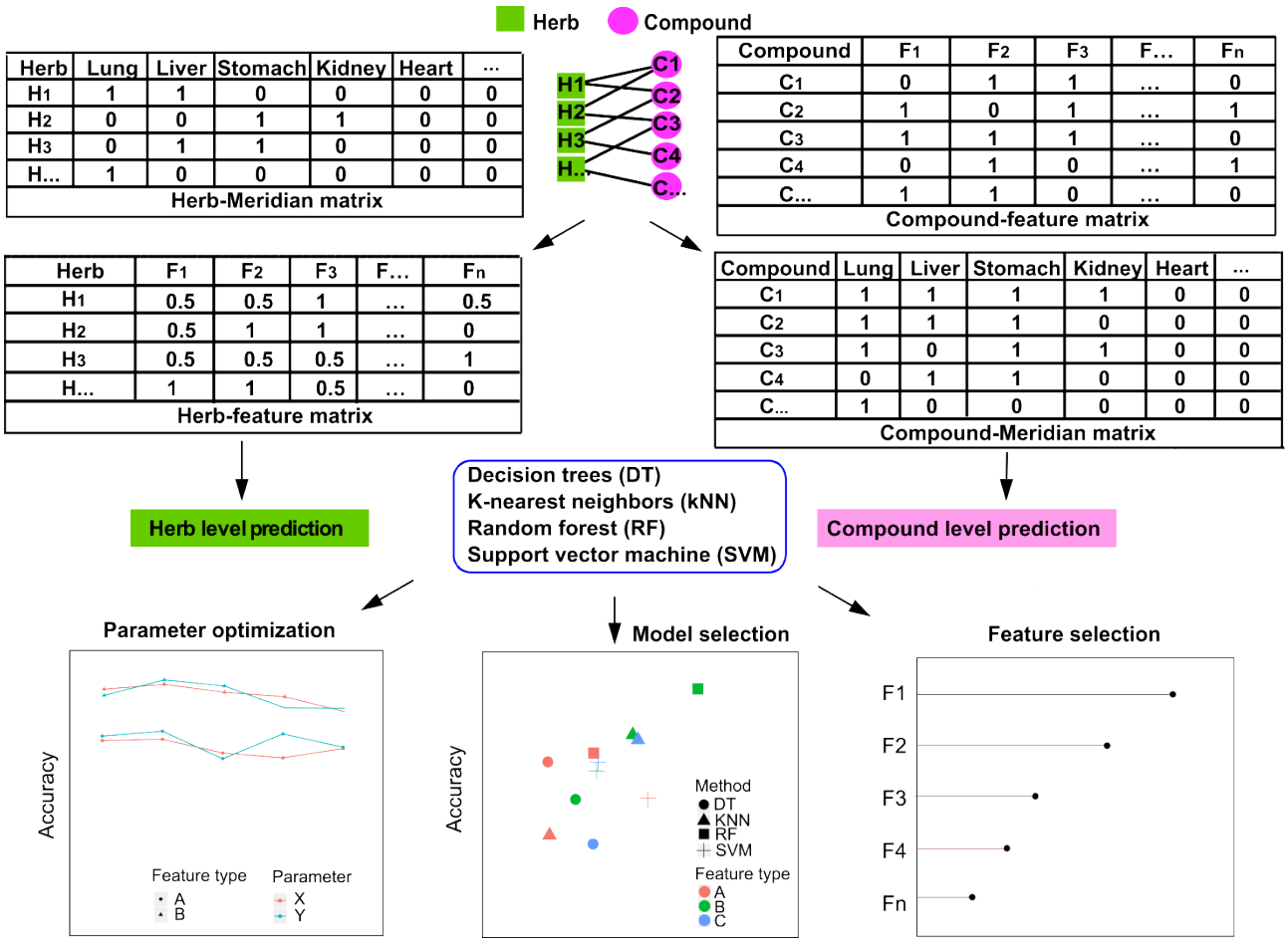

Fig 1. Workflow of the study. Herb-compound network shows the associations between herbs (green rectangles) and their active compounds (purple circles), which were used to determine the Herb-Feature and the Compound-Meridian matrices from the Herb-Meridian and

Compound-Feature matrices. Machine learning methods are utilized to predict the Meridian classes for herbs and compounds respectively, by parameter optimization, model selection and feature selection.

2.1 Data collection

Meridian and ingredient compound information for TCM herbs

We extracted the information of TCM herbs including the Meridian and the chemical components from the newly published database called TCMID [33], which is the largest database of TCM with over 49,000 prescriptions including 8,159 herbs and 25,210 ingredients. However, not all the herbs were included in our data analysis. As the aim of the study was to predict the Meridians based on the structural fingerprints of the herb ingredients, we focused on the herbs with known Meridian information from TCMID. Furthermore, for each herb we included only those ingredient compounds with known SMILES information, such that their structural fingerprints and ADME properties can be determined. The herbs with missing Meridian as well as missing chemical structure information of their ingredient compounds were discarded in this study. The curated dataset contained 18,140 herb-compound pairs including 646 herbs and 10,053 ingredient compounds.

Chemical structural fingerprints for the ingredient compounds

The canonical SMILES representations for the compound structures were determined using Open Babel [34]. We used the PaDEL-Descriptor software [35] to encode SMILES into a list of binary fingerprint features that indicate whether a particular substructure is present or absent in the compound. We considered four common fingerprint types including PubChem

[36], MACCS (Molecular ACCess System) [37], Substructure (Sub) [38] and Extended fingerprint (Ext) [39]. PubChem fingerprint was extracted from the PubChem database (n = 881 bits) while MACCS fingerprint was originated from the cheminformatics system provided by the MDL company (n = 166 bits). Substructure fingerprint was used to represent the specific substructures based on SMARTS Patterns for Functional Group Classification (n = 307 bits) [38],[40]. Extended fingerprint complements the Substructure fingerprint with additional bits describing circular topological features (n = 1024).

ADME properties for the ingredient compounds

ADME properties play important roles to determine the pharmacokinetics of a compound, constituting the key factors that determine the hit and lead optimization processes in drug discovery. ADME properties describe how a compound deposits inside the human body in terms of the processes of absorption, distribution, metabolism and excretion. For instance, water solubility, usually measured as the decimal logarithm of solubility (log S) in the units of mol/l or mg/ml, indicates the maximum dissolvable concentration of a compound in water. After oral administration, a drug reaches the initial portion of the gastrointestinal tract, where the level of gastrointestinal absorption affects the fraction of the drug dose that enters the bloodstream. Lipophilicity, on the other hand, represents the affinity of a compound in a lipophilic environment and thus determines how easily the compound can pass through the lipid membrane of cells. For the TCM herbs, the ADME properties for their ingredient compounds have been largely uncharacterized. Therefore, we resorted to computational methods as an alternative, which have been shown previously to be able to reliably and efficiently determine ADME. For example, the Lipinski's Rule-of-five has been long used for evaluating the bioavailability based on the structure information of compounds [41]. Classical QSAR (Quantitative Structure-Activity Relationship) approaches also rely heavily on

computational prediction of bioactivity properties based on the compound structures [35]. We determined the ADME properties of the ingredient compounds using an online tool SwissADME [42]. In the original publication, the authors of SwissADME showed that the prediction of Lipophilicity achieved an accuracy of r (correlation) = 0.72, MAE (Mean absolute error) = 0.89 and RMSE (root mean square error) = 1.14 against experimental data for 11,993 compounds. SwissADME also showed superior performance on the water solubility prediction with R2 (coefficient of determination) of 0.75, 0.69 and 0.81 based on three different models including the FILTER-IT model [42], the ESOL model [43] and the Ali model [44]. Notably, SwissADME has been recently applied to the study of plant-derived compounds including anticancer polyphenols from *Syzygium alternifolium* [45], PTPN1 (protein tyrosine phosphatase non-receptor type 1) inhibitors from several plant extracts [46] and a TCM called Zhi-zhu Wan [47]. Therefore, we considered the use of SwissADME as a reliable method to probe the ADME properties for TCM herb compounds. The SMILES of each compound was loaded as input to SwissADME, and the result consisted of 36 ADME features including 6 drug likeness features, 5 lipophilicity features, 4 medicinal chemistry features, 9 pharmacokinetics features, 9 physicochemical properties and 3 water solubility properties (**Supplementary Table S1**).

2.2 Construction of Compound-feature matrix and Herb-feature matrix

In this study, the features of a compound were considered as the combination of its fingerprint and ADME features, including 2378 fingerprint features (1024 Ext bits, 881 PubChem bits, 307 Sub bits and 166 MACCS bits) and 36 ADME property features. The four fingerprint types (Ext, PubChem, Sub and MACCS) were first evaluated separately in the machine learning models to determine the best fingerprint type. Then, we combined this best fingerprint type with the ADME features to check whether model performance can be further

improved. The resulting Compound-feature matrix X_C contained 10,053 rows of compounds and 2,414 columns of features.

Based on a previous study, a drug combination's molecular features can be represented by merging the features of its component drugs [48]. We considered also an herb as a mixture of different ingredient compounds, and determined the herb features as below:

Let $\mathbf{C}_j = (c_1, c_2, \ldots, c_k)$ denote the set of ingredient compounds for herb j, where k is the number of compounds. For each compound, its compound feature vector is denoted as $\mathbf{F}_{\text{compound}} = (f_1, f_2, \ldots, f_n)$, where n is the number of features. We modelled the herb feature $\mathbf{F}_{\text{herb}} = (g_1, g_2, \ldots, g_n)$ as the average of its compound features, *i.e.*

$$g_{i,\ i=1,\ldots,n} = \frac{\sum_{c_1, c_2, \ldots, c_k} f_i}{k} \quad (1)$$

As described in section 2.1, we collected 646 herbs and determined 2414 features including 2378 fingerprints and 36 ADME properties for their ingredient compounds. The Herb-feature matrix (HF) thus was size of 646x2414:

$$\mathbf{HF} = \begin{matrix} F_1 \\ F_2 \\ F_3 \\ F_4 \\ \ldots \end{matrix} \begin{bmatrix} 0.2 & 0.1 & 0.3 & 0 & 0 \\ 0 & 0.1 & 0.1 & 0 & 0.8 \\ 0.1 & 0.6 & 0 & 0.1 & 1 \\ 0.5 & 0 & 0.1 & 0.3 & 0.1 \\ 0 & 0.4 & 0.2 & 0 & 0 \end{bmatrix}_{646 \times 2414}$$

Furthermore, to evaluate whether filtering out the compounds with poor ADME properties affects the model prediction, we removed compounds that were predicted with logS lower than -6 by all the three water solubility models (the FILTER-IT model [42], the ESOL model [43] and the Ali model [44]) as well as low gastrointestinal absorption below 30%, which was a commonly accepted threshold to separate well-absorbed from poorly-absorbed compounds. After the filtering, 583 herbs and 4922 compounds were retained. We compared the model prediction accuracies before and after the ADME filtering.

2.3 Construction of Herb-Meridian matrix and Compound-Meridian matrix

TCM herbs can be assigned to one or more of the 12 Meridians as shown in **Table 1**. For each herb, its Meridian vector is denoted as $\mathbf{M}_{\text{herb}} = (m_1, m_2, \ldots, m_{12})$. From the 646 herbs that we collected from TCMID, the Meridian classification for the herbs was represented as a binary Herb-Meridian matrix (HM) for the 12 Meridians as below:

$$\mathbf{HM} = \begin{array}{c} \\ \mathrm{M}_1 \\ \mathrm{M}_2 \\ \mathrm{M}_3 \\ \mathrm{M}_4 \\ \ldots \end{array} \begin{array}{c} \begin{array}{ccccc} \text{Lung} & \text{Spleen} & \text{Stomach} & \text{Kidney} & \ldots \end{array} \\ \begin{bmatrix} 1 & 1 & 0 & 0 & 0 \\ 0 & 1 & 1 & 0 & 0 \\ 1 & 0 & 0 & 1 & 1 \\ 0 & 0 & 1 & 0 & 1 \\ 0 & 0 & 1 & 0 & 0 \end{bmatrix}_{646 \times 12} \end{array}$$

We denoted that $\mathbf{H}_j = (h_1, h_2, \ldots, h_p)$ is a set of p herbs that contain the compound j. The Meridian vector for this compound $\mathbf{M}_{\text{compound}} = (l_1, l_2, \ldots, l_{12})$ was determined as the union of the Meridians of the herbs in H_j, *i.e.*

$$l_{i,\ i=1,\ldots,12} = \mathrm{I}\left(\sum_{h_1, h_2, \ldots, h_p} m_i > 0\right), \tag{2}$$

where $\mathrm{I}(\cdot)$ is an indicator function. The full Compound-Meridian (CM) matrix was constructed accordingly for the 10,053 compounds on the 12 Meridians:

$$\mathbf{CM} = \begin{array}{c} \\ \mathrm{C}_1 \\ \mathrm{C}_2 \\ \mathrm{C}_3 \\ \mathrm{C}_4 \\ \ldots \end{array} \begin{array}{c} \begin{array}{ccccc} \text{Lung} & \text{Spleen} & \text{Stomach} & \text{Kidney} & \ldots \end{array} \\ \begin{bmatrix} 1 & 1 & 0 & 0 & 1 \\ 0 & 1 & 1 & 1 & 1 \\ 1 & 0 & 0 & 1 & 1 \\ 1 & 0 & 1 & 0 & 1 \\ 0 & 0 & 1 & 1 & 0 \end{bmatrix}_{10053 \times 12} \end{array}$$

2.4 Training the machine learning models

We set up the machine learning framework for each Meridian with binary response variables. Four supervised classification methods including SVM, DT, RF and kNN [49] were employed to predict the Meridians. These methods were implemented using the R package caret [50]. SVM

is an algorithm which can determine a hyper plane to maximize the separation between the classes with minimal error. DT constructs a decision tree by representing an observation as a branch node and its classification result by a leave node. kNN is a distance-based learning algorithm where an object is classified according to a majority vote of its neighbors. RF is a decision tree-based ensemble learning approach where each tree votes for its preferred classification and the majority vote classification returns as the final prediction. We used five-fold cross validation to avoid overfitting when evaluating the model performance. Initially the data was split randomly to the training (70%) and testing (30%) sets. A five-fold cross-validation was applied to split the training data randomly into five equally sized folds. At each iteration, one unique fold was hold out while the remaining four folds were used to train a machine learning model. The model performance was then evaluated on the hold-out fold. Such a process was repeated five times, after which the model that produced the highest accuracy was selected as the best model to predict the testing set, which comprise 30% of the total data. The model performance on the independent testing set was reported. The R scripts and input data for the machine learning framework are publically accessible at https://github.com/herb-medicne/meridian-prediction.

2.5 Evaluating the prediction accuracy

We obtained a confusion matrix to evaluate the prediction accuracy for the test data. The overall prediction accuracy was determined using the following equations:

$$\text{overall accuracy} = \frac{\text{TP} + \text{TN}}{\text{TP} + \text{FP} + \text{FN} + \text{TN}} \quad (3)$$

True positive (TP) is the number of positive samples (*i.e.* herbs or compounds) which are correctly identified for a given Meridian. False positive (FP) is the number of positive samples which are not correctly identified. True negative (TN) is the number of negative samples which are correctly identified and false negative (FN) is the number of negative samples

266 which are not correctly identified. To avoid the inflated overall accuracy for imbalanced data,
267 balanced accuracy was also used to evaluate the performance of models, which is the average
268 of sensitivity and specificity:

269 $$\text{balanced accuracy} = \frac{\frac{TP}{TP + FN} + \frac{TN}{FP + TN}}{2} \quad (4)$$

270 Furthermore, Matthews correlation coefficient (MCC) was also utilized for the model
271 evaluation:

272 $$MCC = \frac{TP \times TN - FP \times FN}{\sqrt{(TP + FP)(TP + FN)(TN + FP)(TN + FN)}} \quad (5)$$

273 **2.6 Identification of key features for the prediction of Meridians at the compound level**

274 To find the most important features which play important roles for the Meridian
275 classification, we used the varImp package [51] to estimate the variable importance based on
276 the best models. Furthermore, the SARpy [52] tool was employed to detect key substructures
277 (fragments) that emerge the most frequently as important features when predicting a specific
278 Meridian. SARpy evaluates the significance of each substructure based on the likelihood ratio:

279 $$\text{likelihood ratio} = \frac{TP/FP}{P/N} \quad (6)$$

280 , where TP and FP stand for the number of compounds which contain the substructure
281 and belong, or do not belong to the Meridian, respectively. We selected the top ten
282 important substructures ranked by the likelihood ratio score for each Meridian. These
283 substructures can be therefore considered as the most frequent fragments among the
284 compounds of a specific Meridian.
285

3. Results

3.1 Distribution of Meridians at the herb level and the compound level

In total, 646 herbs including 10,053 ingredient components with Meridian and chemical structure information were obtained from the TCMID database (**Supplementary Table S2**). The Meridian distribution at the herb and the compound levels can be seen in **Fig 2**. At the herb level, altogether 333 herbs target the Liver Meridian, followed by Lung (n = 237), Stomach (n = 235), Spleen (n = 213), Kidney (n = 181), Heart (n = 155) and Large Intestine (n = 111) (**Fig 2A**). In contrast, much less herbs are found for the other five Meridians including Bladder (n = 57), Gallbladder (n = 33), Small Intestine (n = 24), Cardiovascular (n = 4) and Three End (n = 4). Next, we focused on the top seven abundant Meridians including Liver, Lung, Spleen, Stomach, Kidney, Heart and Large Intestine.

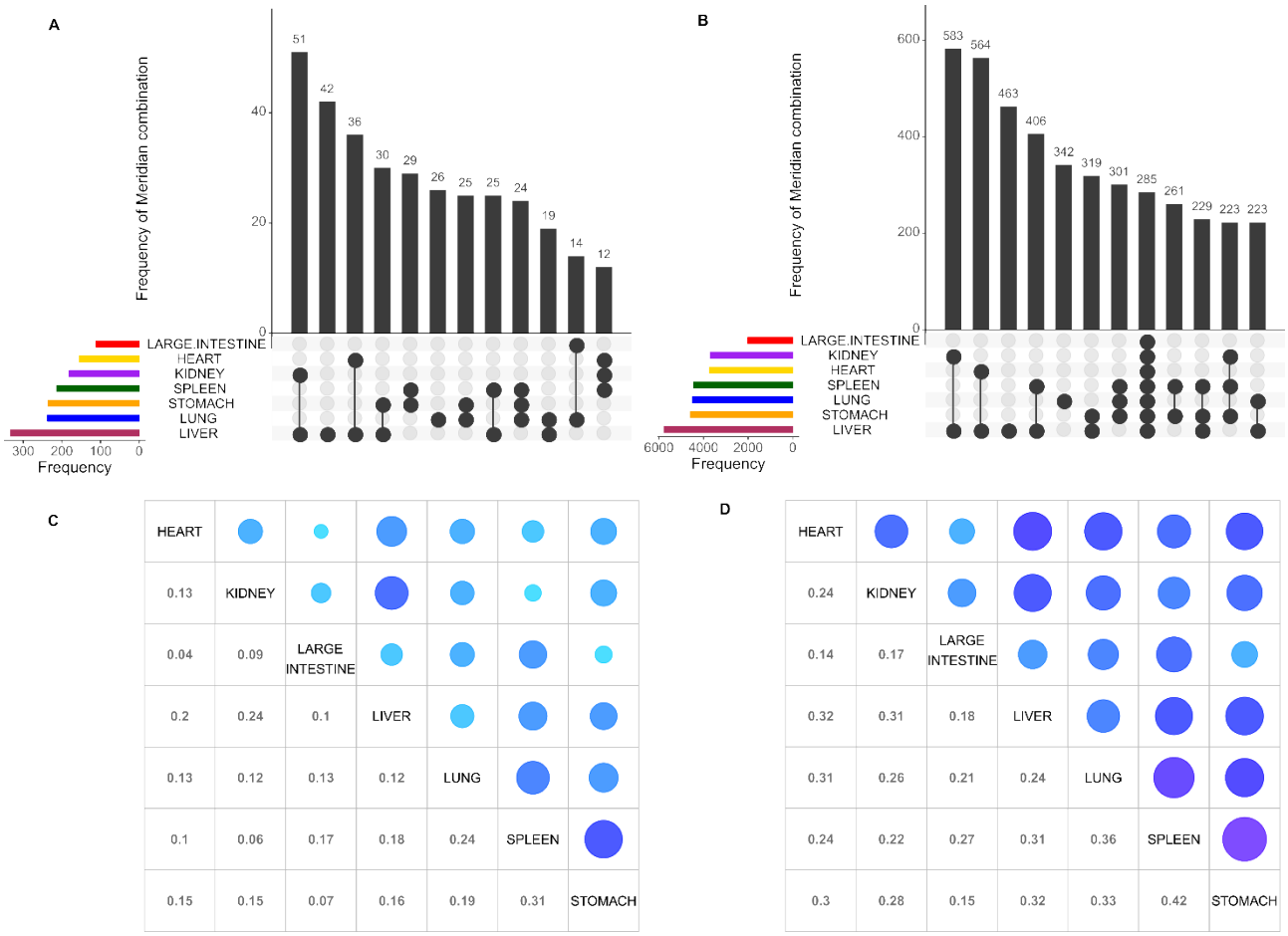

Fig 2. Herb-Meridian and Compound-Meridian distributions. (A-B) The color bars at the bottom left represent the frequency of herbs or compounds for each of the seven major Meridians, which can be further collapsed into subclasses depending on whether an herb or a compound is shared by one or several Meridians. The vertical bars show the frequency of herbs or compounds for a particular subclass of Meridian combination, as indicated by the connected lines below the x-axis between the Meridians. (C-D) The Jaccard coefficients between the Meridian pairs at the herb and the compound levels. The size of blue circles on the upper diagonal shows the degree of the similarity.

As expected, the majority of herbs (n = 580; 89.8%) target more than one Meridian, however, there is a varying degree of overlap between them. It can be seen that Kidney and

Liver has the biggest number of shared herbs (n = 51), followed by 36 herbs that are common between Liver and Heart, and then 30 herbs between Liver and Stomach. The overlap between the Meridians illustrates the multi-target characteristics of TCM herbs. For example, Huo Xiang (*Agastache rugose*) belongs to Lung, Spleen and Stomach simaultensously [53], as this herb is known to relieve the symptoms of Lung, Spleen and Stomach diseases [54]. On the other hand, there are relatively fewer herbs that target only one Meridian. For example, 42 of the 384 (11%) Liver herbs are classified exclusively as Liver herbs and 26 of all the 260 (10%) Lung herbs do not target other Meridians. In contrast, all the herbs that belong to Stomach, Spleen and Large Intestine also target other Meridians. At the compound level, similar patterns was observed, where the Liver Stomach and Lung are again the top abundant Meridians (**Fig 2B**).

In order to quantify the overall similarity between these seven major Meridians, we calculated the Jaccard coefficients using the R package 'Corrplot' [55, 56]. The Jaccard coefficient, also known as Jaccard index, is a measure of overlap between two sets, with a value of zero for complete non-overlap while a value of one for identical sets [57, 58]. As shown in **Fig 2C-D**, the Jaccard coefficients between the Meridians are generally low, with the lowest score found between Heart and Large Intestine (0.04 at the herb level and 0.14 at the compound level), and the highest score found between Spleen and Stomach (0.31 at the herb level and 0.42 at the compound level). The average pairwise Jacaard coefficients are 0.15 and 0.26 for the herb level and for the compound level respectively, indicating that there are weak correlations between Meridians in term of the herb and compound distributions. Therefore, we considered the prediction of each Meridian separately in the following machine learning tasks. Ultimately, for a given new herb or a compound, its Meridians can be predicted using the best machine learning models.

3.2 Prediction accuracy of Meridians using machine learning approaches

We carried out the prediction of Meridians at two data levels including herb level and compound level, for which their features were determined based on structure-based fingerprints and ADME properties. At the herb level, the ADME properties were also utilized to filter out those compounds with low water solubility or low gastrointestinal absorption (see section 2.2 for more details). As a result, only 583 herbs remained after the filtering, covering 4,922 compounds. We evaluated the prediction performance under scenarios of different machine learning methods, feature types and data levels. More specifically, for each one of the seven Meridians, 84 machine learning-based models were constructed including all possible combinations from the four machine learning methods (SVM, DT, RF and kNN), seven feature configurations (Ext, PubChem, Sub, MACCS, ADME, Ext + ADME and All fingerprints + ADME) and three data levels (compound level, herb levels with or without ADME filtering). The model was trained by a five-fold cross validation using 70% data and then tested for its prediction accuracy using the remaining 30% data (see section 2.4 for more details). To benchmark the model performance for each Meridian, we permutated the Meridian labels while keeping the ratio of positive and negative cases unchanged. The model performance for the permutated data was considered as the baseline.

As shown in **Fig 3A**, Large Intestine has the highest overall prediction accuracy among all the seven Meridians (p-value < 0.0001, Wilcoxon rank-sum test), with the median average accuracy reaching 0.83. Model performance for predicting Heart Meridian (median average accuracy at 0.72) became the second best, followed by Kidney (median average accuracy at 0.68). The enhanced overall accuracy for Large Intestine, Heart and Kidney is mainly due to the fewer positive cases at both herb and compound levels (**Fig 2A-B**). Note that we pooled all the 84 machine learning models that differ in their feature combinations and machine learning methods, some of which were sub-optimal and therefore led to poorer prediction

results. Still, these machine learning models performed significantly better than the baseline prediction of permutated models (Fig S1, p-value < 0.0001, Wilcoxon rank-sum test). These results supported the general feasibility of using machine learning approaches to relate chemical information of herbs and compounds to explain Meridians (**Supplementary Table S3**).

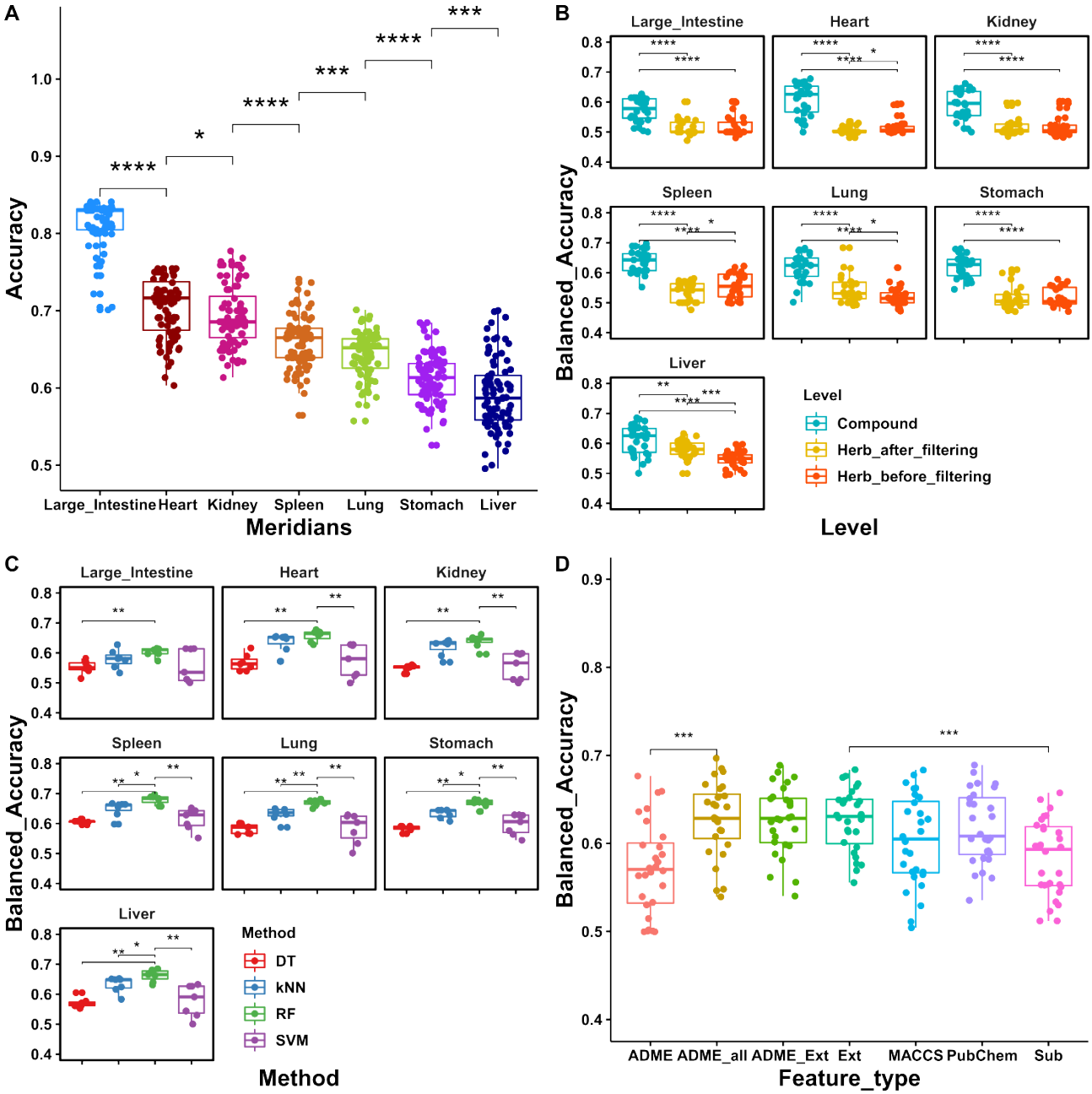

Fig 3. Evaluation of the machine learning model predictions. (A) The overall accuracy for the seven Meridians (B) The balanced accuracy at the three data levels (compound-level, herb-level before and after ADME filtering). (C) The balanced accuracy for the four machine learning methods at the compound level. (D) The balanced accuracy for the ADME and fingerprint feature types at the compound level. Wilcox rank sum test. ns: $p >= 0.05$; *: $p < 0.05$; **: $p < 0.01$; ***: $p < 0.001$; ****: $p < 0.0001$

Furthermore, using the Balanced Accuracy metric, we found that the compound-level prediction performed significantly better than the herb-level predictions (**Fig 3B**, p-value < 0.001, Wilcoxon rank-sum test). At the herb level, filtering out compounds with poor ADME properties improved the prediction significantly in Heart, Lung and Stomach (p-value < 0.05, Wilcoxon rank-sum test), while for Kidney and Spleen only the top machine learning models achieved higher prediction accuracy. In contrast, the ADME filtering seemed not helping the prediction of Large Intestine and Liver Meridians. In order to determine the chemical fingerprint features for an herb, we took the average of its compound features, based on the assumption that all the ingredient compounds are equally contributing to the pharmacology of the herb. This was likely an oversimplification of the actual mechanisms of action for a majority of herbs. However, the biological roles about the ingredient compounds were largely missing from TCMID and other resources, suggesting that the actual contributions of these ingredient compounds have not been thoroughly resolved. In contrast, the compound-level data was more reliable, as each compound was treated independently when determining its molecular features and Meridians. This may explain the superior performance of compound-level predictions compared to the herb-level predictions. We anticipated that the herb-level prediction may be further improved when the actual composition and bioactivity of the

391 compounds can be determined using modern high-throughput techniques e.g. mass
392 spectrometry or HPLC (High performance liquid chromatography) [59].
393 As the compound-level prediction showed better performance than the herb-level
394 prediction, we further compared the prediction accuracy between different machine learning
395 methods at the compound level. As shown in **Fig 3C**, top models of RF performed better than
396 kNN, DT and SVM across all the seven Meridians, suggesting that RF was able to detect the
397 predictive features due to the use of ensemble learning technique. We also evaluated the
398 prediction accuracy of the machine learning methods using different feature types. As shown
399 in **Fig 3D**, models with the Ext fingerprint performed better than the other feature types (p-
400 value <0.05, Wilcoxon rank-sum test). This result was expected as the Ext fingerprint contains
401 1024 bits which are the longest among all the four fingerprint types. Furthermore, models
402 using all the fingerprint types combined with ADME achieved higher top accuracies,
403 compared to the use of them individually (**Fig 3D**). Taken together, we concluded that the
404 combination of all fingerprints with ADME features may carry the most comprehensive
405 information to predict the Meridians at the compound level, for which the RF method
406 achieved the best prediction accuracy compared to other machine learning methods (**Table**
407 **2**).
408
409 **Table 2. The overall prediction accuracy that was achieved for each Meridian at the**
410 **compound level by Random Forest using all the available features.**

Meridian	**Feature**	**Method**	**Accuracy**
Heart	ADME + All fingerprint	RF	0.70
Kidney	ADME + All fingerprint	RF	0.70
Large intestine	ADME + All fingerprint	RF	0.81

Liver	ADME + All fingerprint	RF	0.67
Lung	ADME + All fingerprint	RF	0.65
Spleen	ADME + All fingerprint	RF	0.67
Stomach	ADME + All fingerprint	RF	0.65

411

412 **3.3 Important fingerprint and ADME features to explain Meridian at the compound**
413 **level**

414 After determining RF as the best model, we determined the feature importance score
415 according to its contribution to the change of model prediction accuracy at the compound
416 level: if the removal of a feature resulted in a much worse prediction by the model, then the
417 feature will be given a higher importance score. We selected the top 30 most important
418 features for each Meridian, resulting in 59 unique features in total, including 27 ADME
419 properties and 32 fingerprints. We confirmed that the 59 important features were
420 significantly more predictive than the other features across all the seven Meridians ($p <$
421 0.0001, Wilcoxon rank-sum test), with the median importance score for these 59 top features
422 ranging from 2.77 for Large Intestine to 6.4 for Spleen (**Fig 4A**).

423

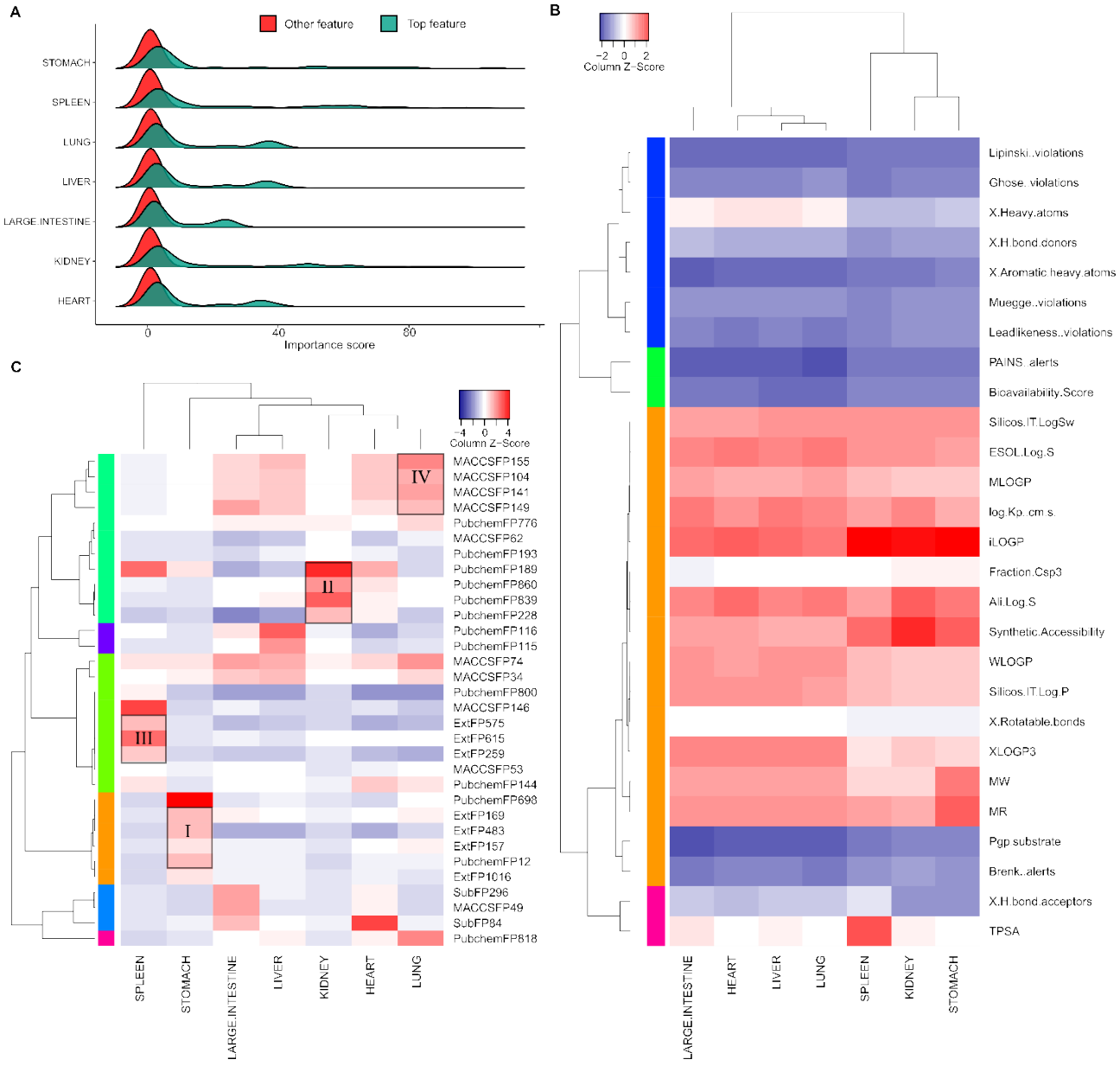

Fig 4. Important features determined at the compound-level prediction of Meridian. (A) The distribution of importance scores for the top 59 features as compared to all features. (B-C) The bi-clustering of the importance scores for the 27 ADME features and 32 fingerprints.

To evaluate the top features across the Meridians, we generated the bi-clustering heatmaps for the top ADME and fingerprint features separately. As shown in **Fig 4B**, lipophilicity features including iLOGP, WLOGP, MLOGP are among the top ADME features across all the seven Meridians, with the mean Z-score of feature importance of 1.66, 0.74 and

433 0.67, separately. This suggested that lipophilicity plays important roles for the Meridian
434 classification of compounds. Molar refractivity (MR), a measure of the total polarizability of a
435 substance, was identified as another important feature (mean Z-score 0.96). In addition,
436 Solubility features predicted by the multiple methods using SwissADME have also shown
437 relatively higher importance, with mean Z-scores ranging from 0.92 to 1.14. Lipophilicity is
438 known to affect pharmacokinetic properties and the overall suitability of drug candidates[60].
439 Molar refractivity and Solubility are known to play important roles for the absorption and
440 subsequent bioavailability of a drug in vivo. Our results suggest the rationale of including the
441 ADME evaluation for understanding the pharmacology and pharmacokinetics of ingredient
442 compounds in herb medicine.

443 We also evaluated the importance scores of the chemical fingerprints. As shown in **Fig**
444 **4C**, the fingerprint features from the same types tend to cluster together, with a Rand Index of
445 0.66 when comparing the similarity between the clustering by cutting the hierarchical tree at
446 1.5 and their actual feature types[61]. For example, the most important fingerprint features
447 for Stomach Meridian formed a cluster (Cluster I in **Fig 4C**), which consisted of mainly Ext
448 fingerprint features (Ext169, Ext483, Ext157 and Ext1016); The most important fingerprint
449 features for Kidney are PubChem fingerprint features (PubChem228, PubChem189,
450 PubChem839 and PubChem860) (Cluster II). Similar patterns were also found for Spleen
451 (Cluster III as an Ext fingerprint dominant cluster) and for Lung (Cluster IV as a MACCS
452 fingerprint dominant cluster). In general, the importance scores for the Ext fingerprints were
453 higher among all the four fingerprint types (**Fig S2**), which is also consistent with the better
454 machine learning performances of Ext fingerprints described earlier in section 3.2 (**Fig 3D**).

455 Finally, we determined the important substructure fragments based on the top
456 fingerprints. As shown in **Supplementary Table S4**, the representative fragments for each
457 Meridian are quite different from each other, which is in line with the limited overlap of herbs

458 between the Meridians (**Fig 2**). This result indicates that there might be enrichment of basic
459 chemical structures that differs between Meridians, which can be further explored using
460 pharmacophore modeling approaches [62].

461 **4. Discussion**

462 Traditional Chinese Medicine (TCM) has gained increasing popularity in the drug discovery
463 field, as shown by a few successful examples including the discovery of artemisinin for
464 treating malaria and arsenic trioxide for treating acute promyelocytic leukemia [63].
465 Currently, there are around 1000 clinical trials on TCM herb medicine registered in the
466 Clinicaltrials.gov [64] (retrieved in January, 2019), suggesting that the therapeutic potential of
467 TCM has been actively researched through more rigorous scientific investigation. While the
468 TCM theory is largely self-consistent as a philosophical narrative, the scientific rationale of
469 why and how it is working remains elusive. For example, the interpretation of five elements
470 and qi is rather metaphysical than physical, which makes many of the TCM concepts difficult
471 to be translated into modern physiological and medical entities [9]. Furthermore, TCMs
472 usually involve many active compounds that modulate various biological targets, where little
473 is known about how these interactions lead to therapeutic relevance under a specific disease
474 context. With the development of molecular profiling technologies, the extraction and
475 characterization of the herb constituents is now possible and is expected to provide a
476 comprehensive source of pharmacology data. Therefore, there have been strong needs for
477 data integration to deconvolute the mechanisms of action of herb medicine in relation to the
478 disease biology, so that a formal framework for testing and understanding of TCM can be
479 established [65].

480 In this study, we built a computational framework to study the concept of Meridians,
481 which has been long established for the classification of TCM herbs and thus constitutes the
482 fundamental basis of treatment strategy in TCM. We collected the Meridian information for

major TCM herbs and determined their features based on the chemical fingerprints and ADME properties. Using supervised classification methods including Random Forests, Support Vector Machines, Decision Trees and K-Nearest Neighbor algorithms, we showed that the Meridians can be accurately predicted especially at the compound level, with an average accuracy of 0.70 of all the Meridians (**Table 2**). Therefore, we concluded that molecular features of the compounds can be considered as the essential information for an herb to be classified as a particular Meridian. In particular, we showed that the ADME properties improved the prediction accuracy, suggesting the relevance and reliability of the in-silico predicted ADME properties for the understanding of Meridians. Ideally, experimentally-validated ADME properties for the ingredient compounds would be needed to confirm the prediction results. Furthermore, we considered 36 ADME features that were provided in SwissADME, assuming that TCM herb compounds become active when absorbed in the bloodstream. However, the therapeutic efficacy of herb medicine may be induced on gut microbiota, which do not necessarily interact with the bloodstream [66]. More relevant factors that may affect the ADME of herb medicine are expected to enhance the model prediction results. On the other hand, we evaluated four major structure-based fingerprint types, and found that the Extended Substructure fingerprints outperformed the other three fingerprint types. This may exemplify the advantage of including more bits in the fingerprint string, as such information may differentiate the complex structure and fragments more distinctively, especially when describing ring structures. In contrast, the MACCS_FP contains only 166 bits which may be insufficient to capture predictive features for this challenging application.

We found that the compound-level prediction is in general more accurate than the herb-level prediction. There might be three reasons for that. Firstly, the exact compound composition for a given herb might not be accurate, as the extraction and detection of active

508 components from herb medicine remains a challenge [67]. Secondly, even though certain
509 compounds can be detected from a given herb, they may not be absorbable due to their poor
510 ADME properties. As a result, the features that were determined for these compounds may
511 play no therapeutic roles and thus do not affect the Meridian of the herbs. Thirdly, although
512 the same compounds can be found from different herbs, their actual abundance may differ. In
513 our construction of binary herb-feature matrix, there is lack of information to differentiate the
514 different levels of compound abundance. We expected the prediction accuracy at the herb
515 level can be improved, providing that more accurate compound composition and activity data
516 become available. In our modeling framework, the extraction of key features at the herb level
517 can be done easily by first extracting the key features at the Compound level, and then
518 combining them for a particular herb, using the Compound-Feature matrix and Herb-
519 Compound matrix. With this framework, we may predict not only the Meridian for new herbs,
520 but also for approved synthetic compounds for which their disease indications are already
521 known. The link between Meridian and disease indications may provide more physiological
522 understanding of Meridian.

523 We identified that Random Forest (RF) as the best classification method, corroborating
524 the superior performance of RF in similar machine learning tasks [68]. As an Ensemble
525 Learning method, RF averaged the predictions from multiple decision trees and thus lowered
526 the risk of overfitting. In the future, more advanced machine learning methods such as Deep
527 Learning may be worth trying [69]. To make sense of TCM, the ultimate objective is not only a
528 predictive model but also an interpretable model that can help understand the underlying
529 mechanisms of action. Here, we identified the predictive features that may provide initial
530 evidence for the molecular basis of Meridians, which may facilitate the discovery of novel
531 active compounds from TCM herbs. By further improving the knowledge of active ingredients
532 for TCM herbs and the accuracy of machine learning algorithms, we expected that the

533 computational framework can be greatly expanded towards a more systematic understanding
534 of Meridians.

535 TCMID is currently the largest database of TCM that collects over 49,000 prescriptions
536 including 8,159 herbs and 25,210 ingredients. However, the majority of these herbs are lack
537 of appropriate annotation on their Meridian information, highlighting the limited
538 understanding of the topic. We extracted a subset of herbs from TCMID (n = 646) with known
539 Meridian information and then included their ingredient compounds with known chemical
540 structures (n = 10,053), with which the most predictive machine learning models and features
541 were determined. To be able utilize our machine learning framework to predict the unknown
542 Meridian for a given herb, the structural information of its ingredient compounds need to be
543 provided as input data. With the structural information it is then possible to determine the
544 fingerprint and ADME features. In the future, we envisage that more comprehensive
545 structural information about the active ingredients in herbs can be determined, so that the
546 Meridian annotation of herbs can be done more systematically and more accurately. The
547 advanced machine learning approaches that are tailored for analyzing such complex datasets
548 may hold the key to the understanding of TCM rationale, which may ultimately provide novel
549 insights for drug discovery and disease treatment [62].

550 **Acknowledgements**

551 We thank the authors of the TCMID database for making the herb medicine annotation data
552 fully accessible.

553 **References**

554 1. A Antolin A, Workman P, Mestres J, Al-Lazikani B. Polypharmacology in precision
555 oncology: current applications and future prospects. Curr Pharm Des. 2016;22(46):6935-45.

556 2. Tschöp MH, Finan B, Clemmensen C, Gelfanov V, PerezTilve D, Müller TD, et al.
557 Unimolecular polypharmacy for treatment of diabetes and obesity. Cell Metab. 2016;24(1):51-
558 62.
559 3. Reddy AS, Zhang S. Polypharmacology: drug discovery for the future. Expert Rev
560 Clin Pharmacol. 2013;6(1):41-7.
561 4. Li S, Zhang B, Jiang D, Wei Y, Zhang N. Herb network construction and co-module
562 analysis for uncovering the combination rule of traditional Chinese herbal formulae. BMC
563 Bioinformatics. 2010;11(11):S6.
564 5. Zhao X, Zheng X, Fan T, Li Z, Zhang Y, Zheng J. A novel drug discovery strategy
565 inspired by traditional medicine philosophies. Science. 2015;347(6219):S38-S40.
566 6. Liang H, Ruan H, Ouyang Q, Lai L. Herb-target interaction network analysis helps
567 to disclose molecular mechanism of traditional Chinese medicine. Sci Rep. 2016;6:36767.
568 7. Zhang C, Li L, Zhang G, Chen K, Lu A. Deciphering Potential Correlations between
569 New Biomarkers and Pattern Classification in Chinese Medicine by Bioinformatics: Two
570 Examples of Rheumatoid Arthritis. Chin J Integr Med. 2018. doi: http://sci-
571 hub.tw/10.1007/s11655-018-2571-8.
572 8. Chan K. Progress in traditional Chinese medicine. Trends Pharmacol Sci.
573 1995;16(6):182-7.
574 9. Gu S, Pei J. Innovating Chinese Herbal Medicine: From Traditional Health Practice
575 to Scientific Drug Discovery. Front Pharmacol. 2017;8:381.
576 10. Rezadoost H, Karimi M, Jafari M. Proteomics of hot-wet and cold-dry
577 temperaments proposed in Iranian traditional medicine: a Network-based Study. Sci Rep.
578 2016;6:30133.

579 11. Jafari M, Rezadoost H, Karimi M, Mirzaie M, Rezaie-Tavirani M, Khodabandeh M, et
580 al. Proteomics and traditional medicine: new aspect in explanation of temperaments.
581 Complement Med Res. 2014;21(4):250-3.
582 12. Chon TY, Lee MC. Acupuncture Mayo Clinic proceedings. 2013;88(10):1141-6.
583 13. Azizkhani M, Dastjerdi MV, Arani MT, Pirjani R, Sepidarkish M, Ghorat F, et al.
584 Traditional Dry Cupping Therapy Versus Medroxyprogesterone Acetate in the Treatment of
585 Idiopathic Menorrhagia: A Randomized Controlled Trial. Iran Red Crescent Med J.
586 2018;20(2):e60508. doi: 10.5812/ircmj.60508.
587 14. Wang G, Ayati MH, Zhang W. Meridian studies in China: a systematic review. J
588 Acupunct Meridian Stud. 2010;3(1):1-9.
589 15. Longhurst JC. Defining meridians: a modern basis of understanding. J Acupunct
590 Meridian Stud. 2010;3(2):67-74.
591 16. Bai Y, Wang J, Wu J, Dai J, Sha O, Tai Wai Yew D, et al. Review of evidence suggesting
592 that the fascia network could be the anatomical basis for acupoints and meridians in the human
593 body. Evid Based Complement Alternat Med. 2011;2011:6. doi: 10.1155/2011/260510.
594 17. Ma W, Tong H, Xu W, Hu J, Liu N, Li H, et al. Perivascular space: possible anatomical
595 substrate for the meridian. Journal of alternative and complementary medicine. 2003;9(6):851-
596 9.
597 18. Chen C, Zhang D. Anti-inflammatory effects of 81 Chinese herb extracts and their
598 correlation with the characteristics of traditional Chinese medicine. Evid Based Complement
599 Alternat Med. 2014;2014:8. doi: http://sci-hub.tw/10.1155/2014/985176.
600 19. Jie Z, Lin T, Qian G, Jingyan M. General Medication Rules in Treating Spleen-
601 stomach Disharmony Based on Traditional Chinese Medicine Inheritance Platform. World
602 Chinese Medicine. 2016;1:048.

603 20. Cheng J. Chinese Herbal Medicine: Perspectives. Herbal Medicines: Springer; 2016.
604 p. 225-35.
605 21. Fu X, Liu H, Wang P, Guan H. A study on the antioxidant activity and tissues
606 selective inhibition of lipid peroxidation by saponins from the roots of Platycodon grandiflorum.
607 Am J Chin Med. 2009;37(05):967-75.
608 22. Wang X, MorrisNatschke SL, Lee K. New developments in the chemistry and
609 biology of the bioactive constituents of Tanshen. Med Res Rev. 2007;27(1):133-48.
610 23. Li Z, Xu S, Liu P. Salvia miltiorrhiza Burge (Danshen): A golden herbal medicine in
611 cardiovascular therapeutics. Acta Pharmacol Sin. 2018;39:802-24.
612 24. Huang C, Zheng C, Li Y, Wang Y, Lu A, Yang L. Systems pharmacology in drug
613 discovery and therapeutic insight for herbal medicines. Brief Bioinform. 2013;15(5):710-33.
614 25. Yang X, Qi M, Li Q, Chen L, Yu Z, Yang L. Information integration research on
615 cumulative effect of 'Siqi, Wuwei, and Guijing'in Traditional Chinese Medicine. J Tradit Chin Med.
616 2016;36(4):538-46.
617 26. Fu X, Mervin LH, Li X, Yu H, Li J, Mohamad Zobir SZ, et al. Toward understanding
618 the cold, hot, and neutral nature of Chinese Medicines using in silico mode-of-action analysis. J
619 Chem Inf Model. 2017;57(3):468-83.
620 27. Wang M, Li L, Yu C, Yan A, Zhao Z, Zhang G, et al. Classification of Mixtures of
621 Chinese Herbal Medicines Based on a Self-Organizing Map (SOM). Mol Inform.
622 2016;35(3-4):109-15.
623 28. Cortes C, Vapnik V. Support vector networks. Mach Learn. 1995;20:273-97.
624 29. Quinlan JR. C4. 5: programs for machine learning: Elsevier; 2014.
625 30. Liaw A, Wiener MJRn. Classification and regression by randomForest.
626 2002;2(3):18-22.
627 31. Breiman L. Random forests. Mach Learn. 2001;45(1):5-32.

628 32. Zhang H, Berg AC, Maire M, Malik J, editors. SVM-KNN: Discriminative nearest
629 neighbor classification for visual category recognition. Computer Vision and Pattern
630 Recognition, 2006 IEEE Computer Society Conference on; 2006: IEEE.
631 33. Huang L, Xie D, Yu Y, Liu H, Shi Y, Shi T, et al. TCMID 2.0: a comprehensive resource
632 for TCM. Nucleic acids research. 2017;46(D1):D1117-D20.
633 34. O'Boyle NM, Banck M, James CA, Morley C, Vandermeersch T, Hutchison GR. Open
634 Babel: An open chemical toolbox. J Cheminform. 2011;3(1):33.
635 35. Yap CW. PaDEL-descriptor: An open source software to calculate molecular
636 descriptors and fingerprints. J Comput Chem. 2011;32(7):1466-74.
637 36. Han L, Wang Y, Bryant SH. Developing and validating predictive decision tree
638 models from mining chemical structural fingerprints and high–throughput screening data in
639 PubChem. J BMC bioinformatics. 2008;9(1):401.
640 37. Durant JL, Leland BA, Henry DR, Nourse JG. Reoptimization of MDL keys for use in
641 drug discovery. J Chem Inf Comput Sci. 2002;42(6):1273-80.
642 38. Hall LH, Kier LB. Electrotopological state indices for atom types: a novel
643 combination of electronic, topological, and valence state information. J Chem Inf Comput Sci.
644 1995;35(6):1039-45.
645 39. Rogers D, Hahn M. Extended-connectivity fingerprints. J Chem Inf Model.
646 2010;50(5):742-54.
647 40. http://www.daylight.com/dayhtml/doc/theory/theory.smarts.html.
648 41. Lipinski CA, Lombardo F, Dominy BW, Feeney PJ. Experimental and computational
649 approaches to estimate solubility and permeability in drug discovery and development settings.
650 Adv Drug Deliv Rev. 1997;23(1-3):3-25.

651 42. Daina A, Michielin O, Zoete V. SwissADME: a free web tool to evaluate
652 pharmacokinetics, drug-likeness and medicinal chemistry friendliness of small molecules. Sci
653 Rep. 2017;7:42717.
654 43. Delaney JS. ESOL: estimating aqueous solubility directly from molecular structure.
655 J Chem Inf Comput Sci. 2004;44(3):1000-5.
656 44. Ali J, Camilleri P, Brown MB, Hutt AJ, Kirton SB. Revisiting the General Solubility
657 Equation: In Silico Prediction of Aqueous Solubility Incorporating the Effect of Topographical
658 Polar Surface Area. J Chem Inf Model. 2012;52(2):420-8.
659 45. Yugandhar P, Kumar KK, Neeraja P, Savithramma N. Isolation, characterization and
660 in silico docking studies of synergistic estrogen receptor a anticancer polyphenols from
661 Syzygium alternifolium (Wt.) Walp. J Intercult Ethnopharmacol. 2017;6(3):296.
662 46. Bibi S, Sakata K. An Integrated Computational Approach for Plant-Based Protein
663 Tyrosine Phosphatase Non-Receptor Type 1 Inhibitors. Curr Comput Aided Drug Des.
664 2017;13(4):319-35.
665 47. Wang C, Ren Q, Chen X-T, Song Z-Q, Ning Z-C, Gan J-H, et al. System pharmacology-
666 based strategy to decode the synergistic mechanism of Zhi-zhu Wan for functional dyspepsia.
667 Front Pharmacol. 2018;9:841.
668 48. Mason DJ, Stott I, Ashenden S, Weinstein ZB, Karakoc I, Meral S, et al. Prediction of
669 antibiotic interactions using descriptors derived from molecular structure. J Med Chem.
670 2017;60(9):3902-12.
671 49. Wang Q, Li X, Yang H, Cai Y, Wang Y, Wang Z, et al. In silico prediction of serious
672 eye irritation or corrosion potential of chemicals. RSC Adv. 2017;7(11):6697-703.
673 50. Kuhn M. Caret package. J Stat Softw. 2008;28(5):1-26.
674 51. Gevrey M, Dimopoulos I, Lek S. Review and comparison of methods to study the
675 contribution of variables in artificial neural network models. Ecol Modell. 2003;160(3):249-64.

676 52. Ferrari T, Cattaneo D, Gini G, Golbamaki Bakhtyari N, Manganaro A, Benfenati E.
677 Automatic knowledge extraction from chemical structures: the case of mutagenicity prediction.
678 SAR QSAR Environ Res. 2013;24(5):365-83.
679 53. Xue X, Huang X, Gao N, Liu E, Ren L-y. Effects of Huoxiang Zhengqi Liquid on
680 Expression of ZO-1 in Ileum Mucosa of Rats with Dampness Retention Syndrome. Chinese
681 Journal of Experimental Traditional Medical Formulae. 2011;16:069.
682 54. Committee NP. Pharmacopoeia of the People's Republic of China. Part.
683 2010;1:392-3.
684 55. Friendly M. Corrgrams: Exploratory displays for correlation matrices. Am Stat.
685 2002;56(4):316-24.
686 56. Wei T, Simko V. corrplot: Visualization of a correlation matrix. R package version
687 073. 2013;230(231):11.
688 57. Niwattanakul S, Singthongchai J, Naenudorn E, Wanapu S. Using of Jaccard
689 coefficient for keywords similarity. Proceedings of the International MultiConference of
690 Engineers and Computer Scientists2013. p. 380-4.
691 58. Jafari M, Mirzaie M, Sadeghi M. Interlog protein network: an evolutionary
692 benchmark of protein interaction networks for the evaluation of clustering algorithms. BMC
693 Bioinformatics. 2015;16(1):319.
694 59. Zhang A, Sun H, Wang X. Mass spectrometry-driven drug discovery for
695 development of herbal medicine. Mass Spectrom Rev. 2018;37(3):307-20.
696 60. Kubinyi H. Lipophilicity and drug activity. Progress in Drug Research/Fortschritte
697 Der Arzneimittelforschung/Progrès Des Recherches Pharmaceutiques: Springer; 1979. p. 97-
698 198.

699 61. Yeung KY, Ruzzo WL. Details of the adjusted rand index and clustering algorithms,
700 supplement to the paper an empirical study on principal component analysis for clustering
701 gene expression data. Bioinformatics. 2001;17(9):763-74.
702 62. Rodrigues T, Reker D, Schneider P, Schneider G. Counting on natural products for
703 drug design. Nat Chem. 2016;8(6):531.
704 63. Z X. Modernization: One step at a time. Nature. 2011;480(7378):S90-2.
705 64. Zarin DA, Tse T, Williams RJ, Califf RM, Ide NC. The ClinicalTrials. gov results
706 database—update and key issues. The New England journal of medicine. 2011;364(9):852-60.
707 65. Fung FY, Linn YC, Medicine A. Developing traditional Chinese medicine in the era
708 of evidence-based medicine: current evidences and challenges. Evid Based Complement
709 Alternat Med. 2015;2015:9.
710 66. Zhou S-S, Xu J, Zhu H, Wu J, Xu J-D, Yan R, et al. Gut microbiota-involved
711 mechanisms in enhancing systemic exposure of ginsenosides by coexisting polysaccharides in
712 ginseng decoction. Sci Rep. 2016;6:22474.
713 67. Zhang Q, Lin L, Ye W. Techniques for extraction and isolation of natural products:
714 a comprehensive review. Chinese medicine. 2018;13(1):20.
715 68. Svetnik V, Liaw A, Tong C, Culberson JC, Sheridan RP, Feuston BP. Random forest:
716 a classification and regression tool for compound classification and QSAR modeling. J Chem Inf
717 Comput Sci. 2003;43(6):1947-58.
718 69. Gawehn E, Hiss JA, Schneider G. Deep learning in drug discovery. Mol Inform.
719 2016;35(1):3-14.

720

721

Supporting information

Fig S1. Model performance of Random Forest on the real data as compared to permutated data at compound and herb levels. ****: p-value < 0.0001.

Fig S2. The importance scores grouped by the feature types according to Random Forest predictions for the seven Meridians at the compound level.

Supplementary Table 1. The 36 ADME properties based on the chemical structure of compounds.

Supplementary Table 2. The Meridians and other TCM annotations for the 646 herbs.

Supplementary Table 3. The prediction performances for the combinations of data levels, feature types and machine learning methods.

Supplementary Table 4. Top 30 important ADME features, fingerprint bits and important substructure fragments for each Meridian determined at the compound level.

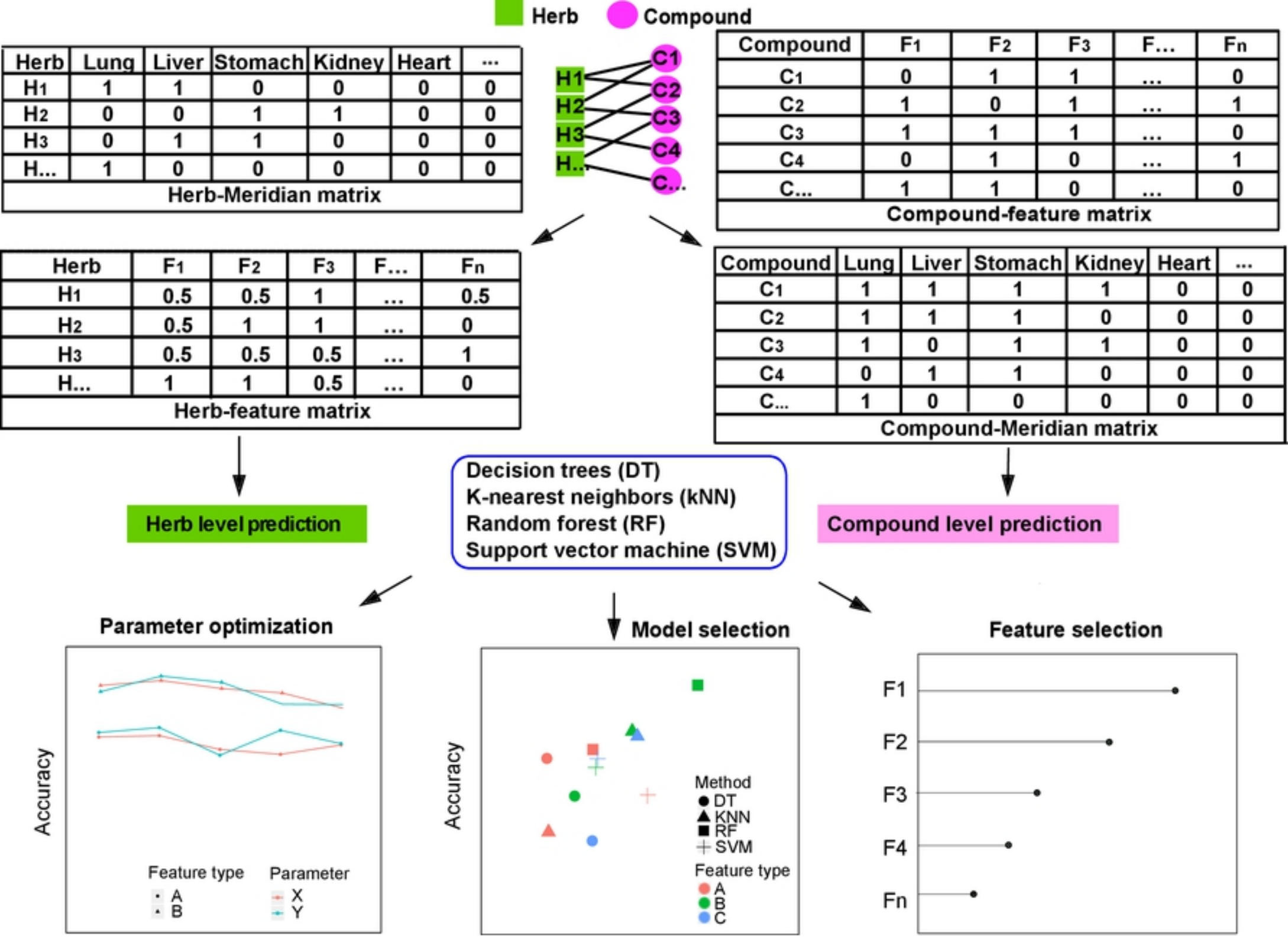
Herb
Compound
Herb | Lung | Liver | Stomach | Kidney | Heart | ...
H1 | 1 | 1 | 0 | 0 | 0 | 0
H2 | 0 | 0 | 1 | 1 | 0 | 0
H3 | 0 | 1 | 1 | 0 | 0 | 0
H... | 1 | 0 | 0 | 0 | 0 | 0
Herb-Meridian matrix
H1
H2
H3
H...
C1
C2
C3
C4
C...
Compound | F1 | F2 | F3 | F... | Fn
C1 | 0 | 1 | 1 | ... | 0
C2 | 1 | 0 | 1 | ... | 1
C3 | 1 | 1 | 1 | ... | 0
C4 | 0 | 1 | 0 | ... | 1
C... | 1 | 1 | 0 | ... | 0
Compound-feature matrix
Herb | F1 | F2 | F3 | F... | Fn
H1 | 0.5 | 0.5 | 1 | ... | 0.5
H2 | 0.5 | 1 | 1 | ... | 0
H3 | 0.5 | 0.5 | 0.5 | ... | 1
H... | 1 | 1 | 0.5 | ... | 0
Herb-feature matrix
Compound | Lung | Liver | Stomach | Kidney | Heart | ...
C1 | 1 | 1 | 1 | 1 | 0 | 0
C2 | 1 | 1 | 1 | 0 | 0 | 0
C3 | 1 | 0 | 1 | 1 | 0 | 0
C4 | 0 | 1 | 1 | 0 | 0 | 0
C... | 1 | 0 | 0 | 0 | 0 | 0
Compound-Meridian matrix
Herb level prediction
Decision trees (DT)
K-nearest neighbors (kNN)
Random forest (RF)
Support vector machine (SVM)
Compound level prediction
Parameter optimization
Accuracy
Feature type
A
B
Parameter
X
Y
Model selection
Accuracy
Method
DT
KNN
RF
SVM
Feature type
A
B
C
Feature selection
F1
F2
F3
F4
Fn

Figure1

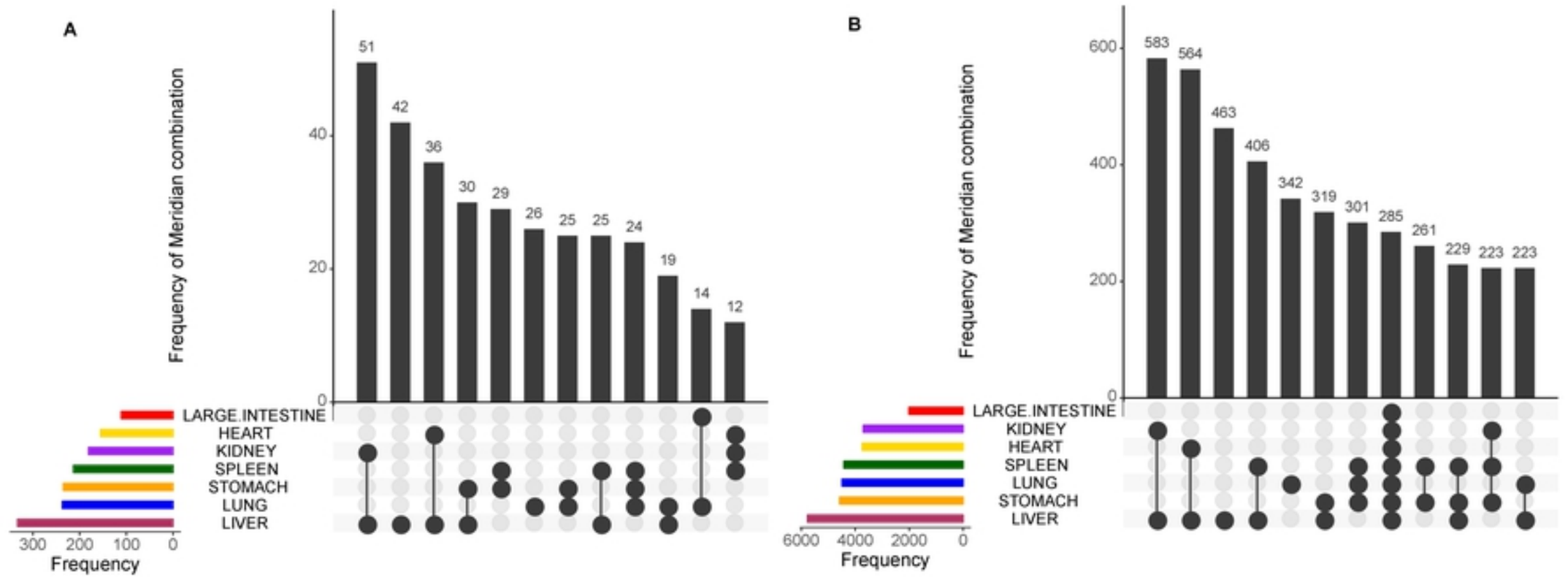

C

HEART						
0.13	KIDNEY					
0.04	0.09	LARGE INTESTINE				
0.2	0.24	0.1	LIVER			
0.13	0.12	0.13	0.12	LUNG		
0.1	0.06	0.17	0.18	0.24	SPLEEN	
0.15	0.15	0.07	0.16	0.19	0.31	STOMACH

D

HEART						
0.24	KIDNEY					
0.14	0.17	LARGE INTESTINE				
0.32	0.31	0.18	LIVER			
0.31	0.26	0.21	0.24	LUNG		
0.24	0.22	0.27	0.31	0.36	SPLEEN	
0.3	0.28	0.15	0.32	0.33	0.42	STOMACH

Figure2

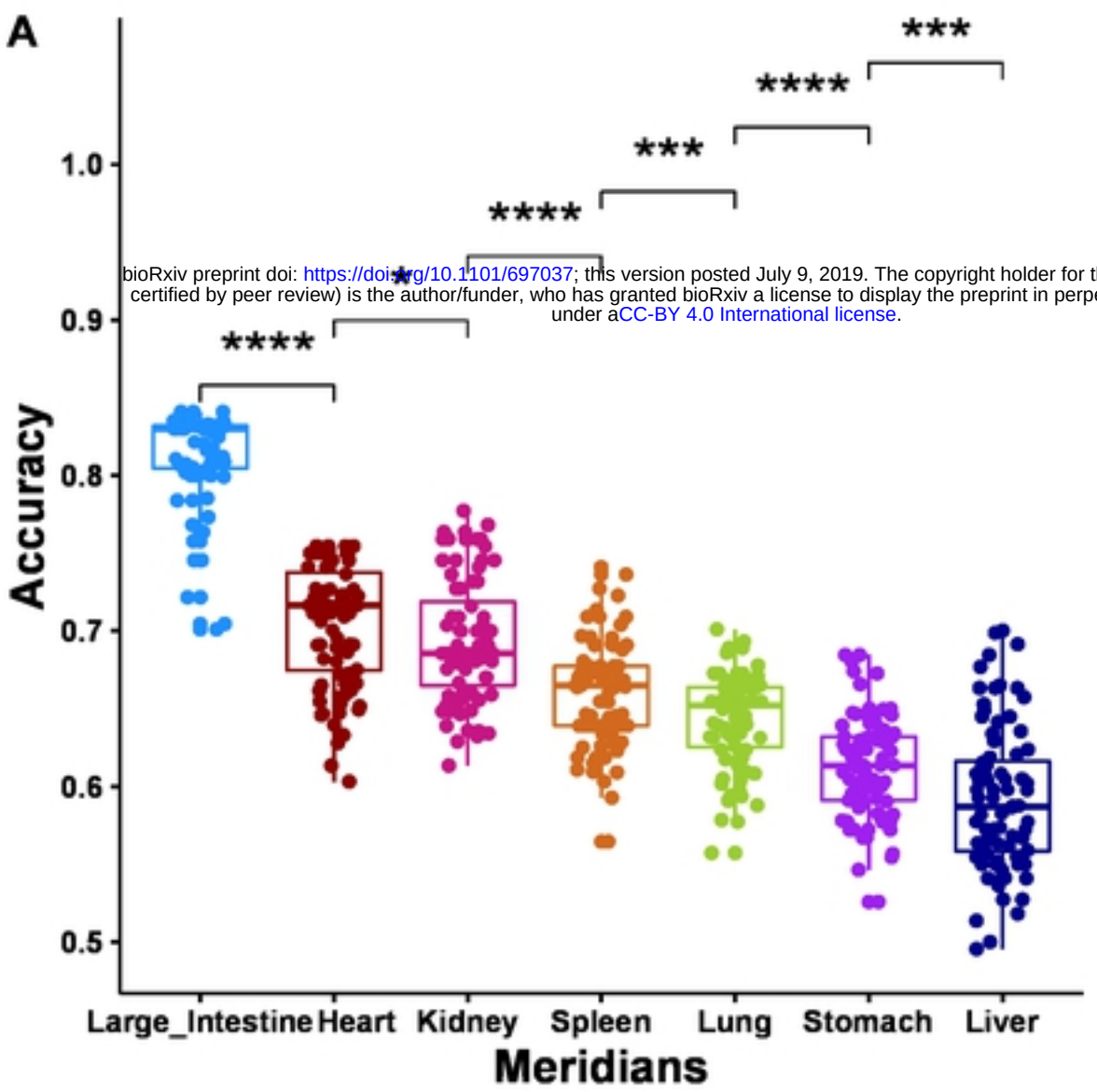

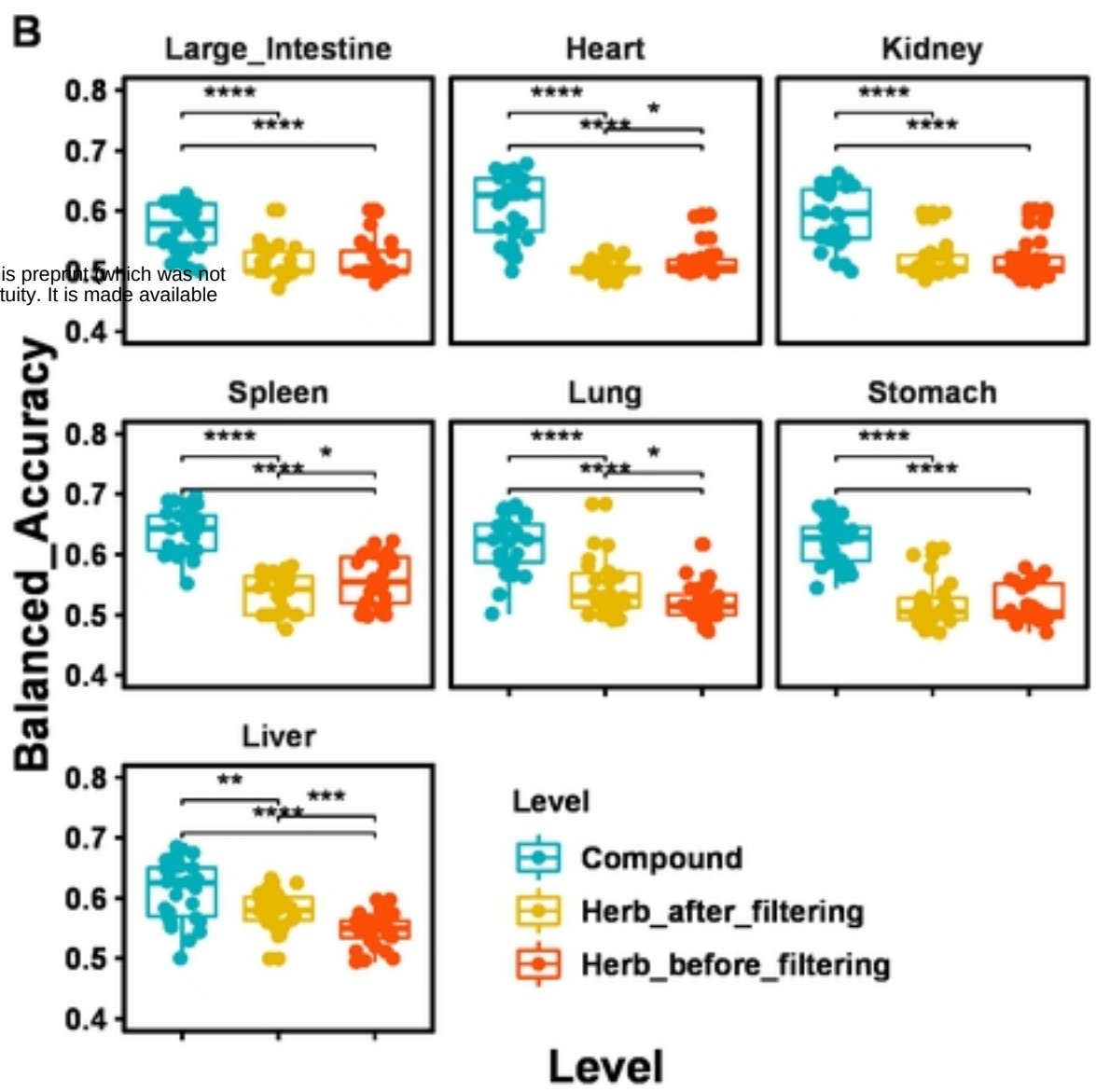

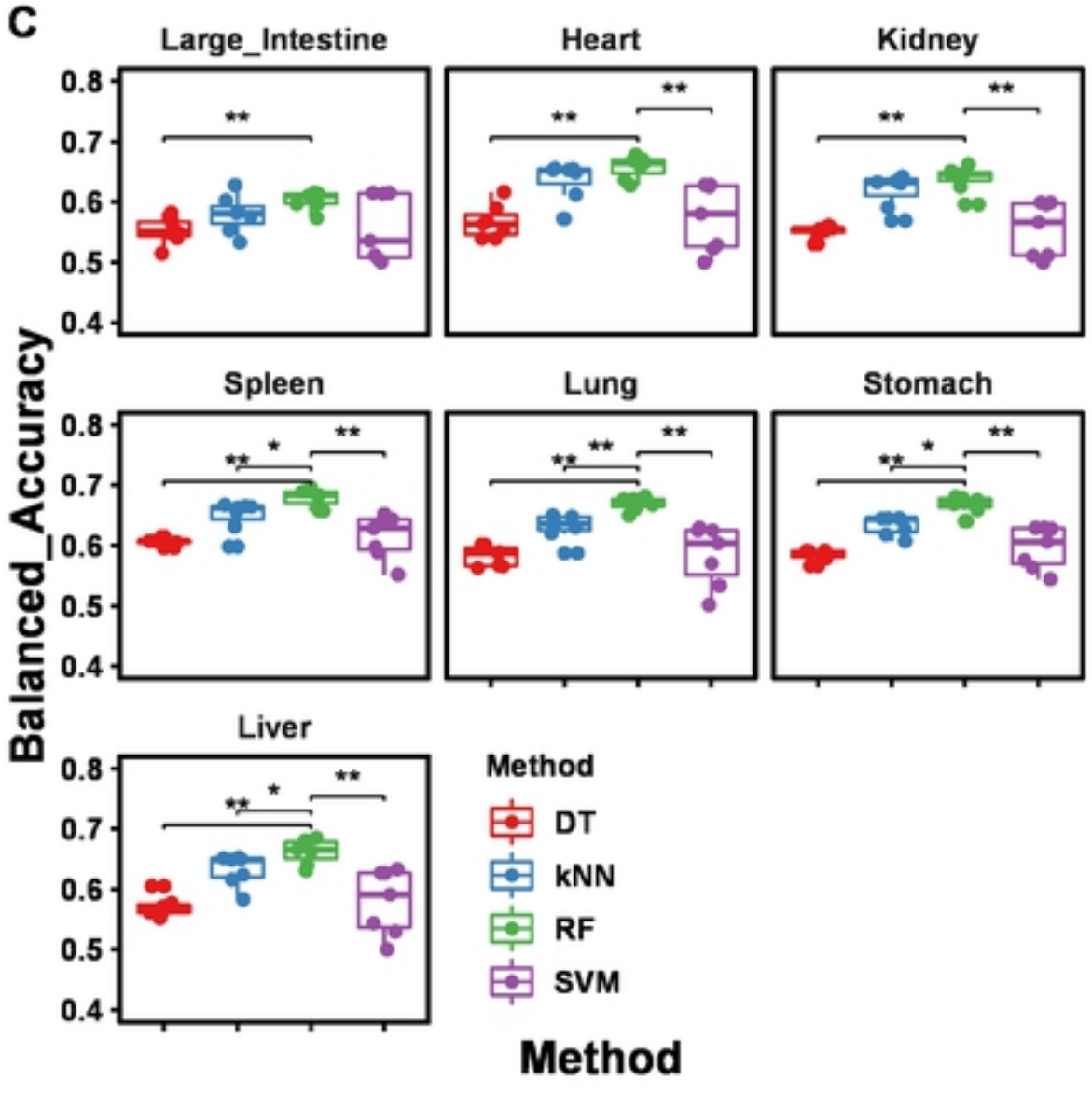

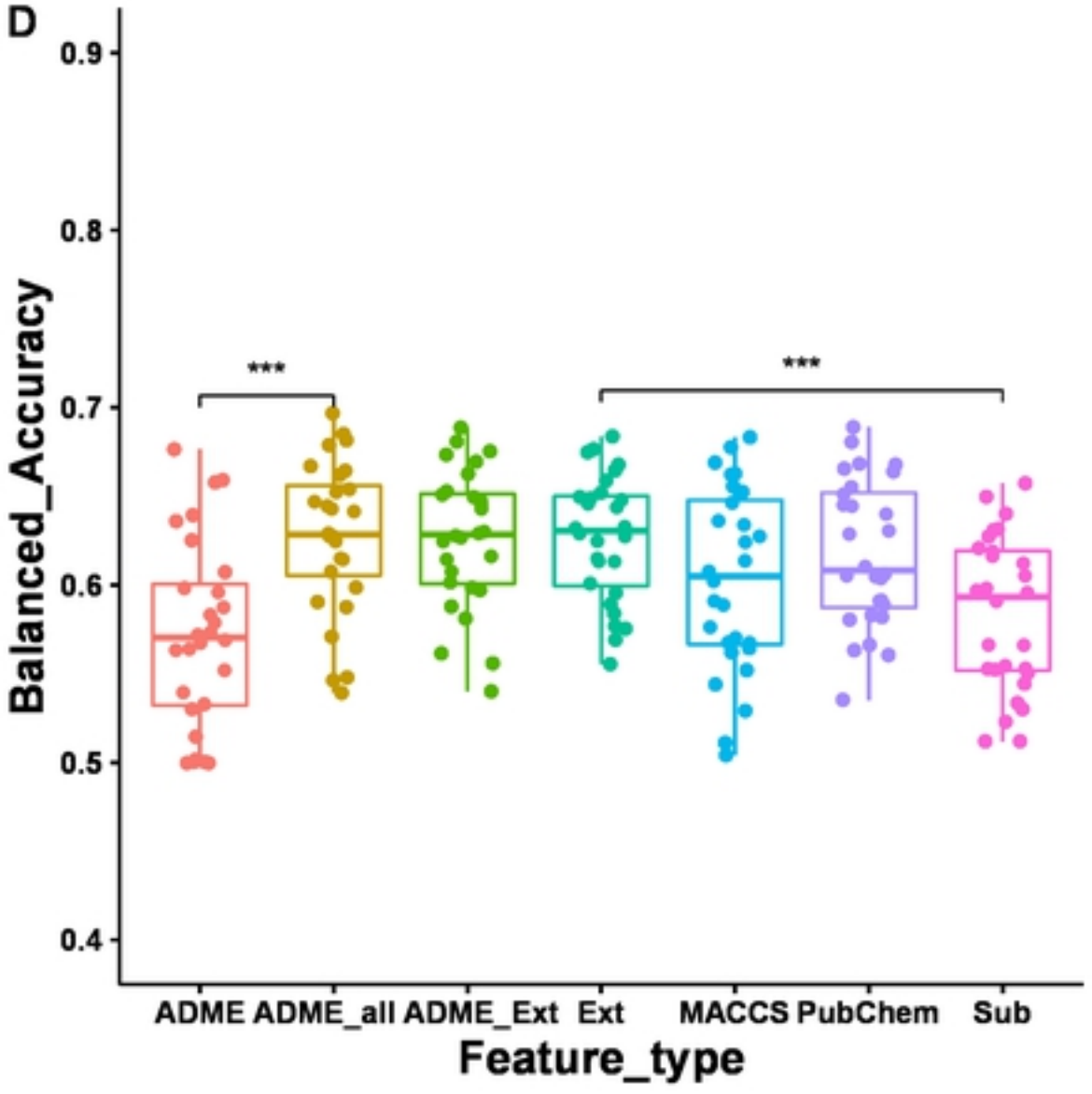

Figure3

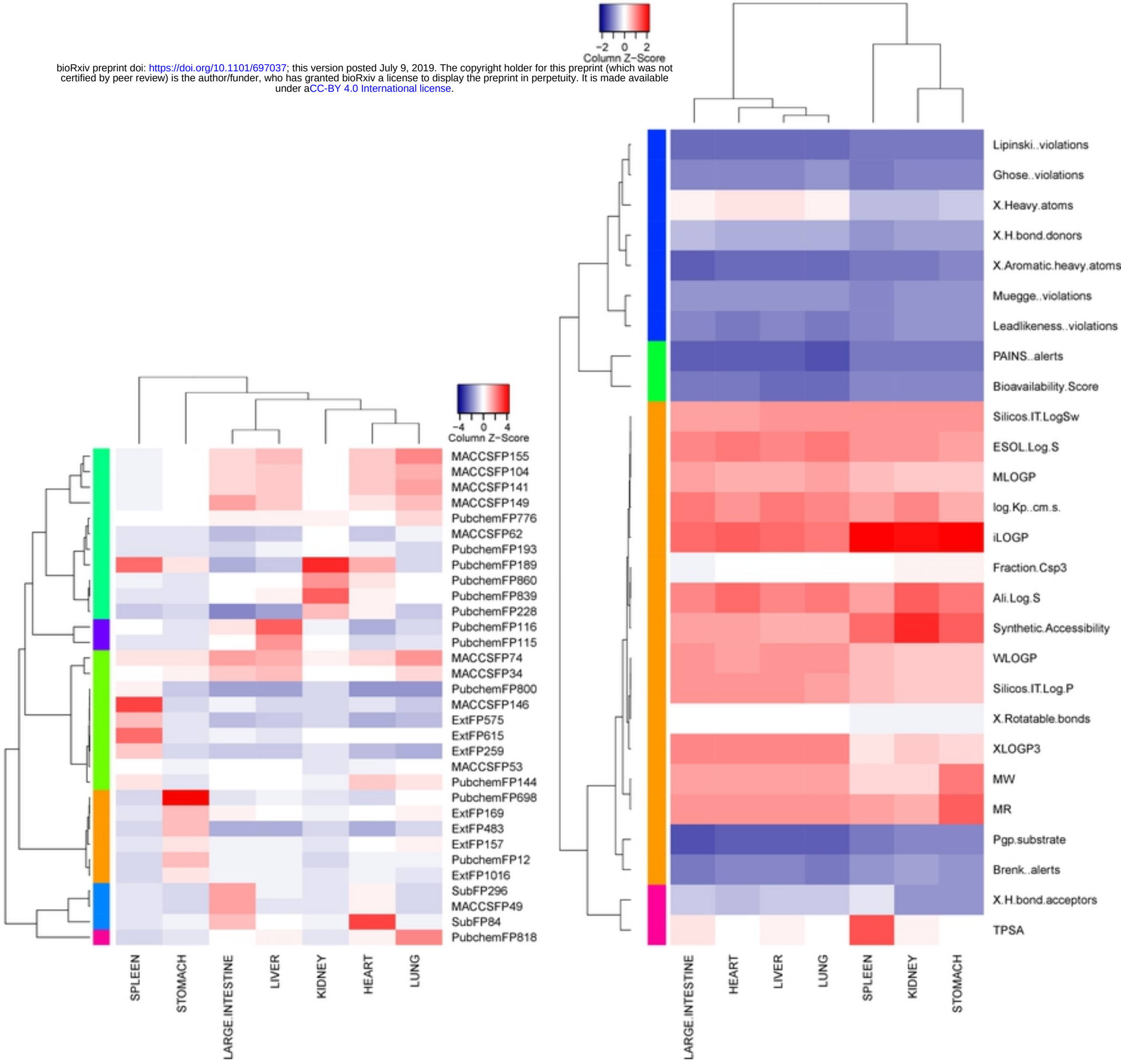

Figure4